Composites Part C: Open Access 3 (2020) 100075

Contents lists available at ScienceDirect

Composites Part C: Open Access

journal homepage: www.elsevier.com/locate/jcomc

Enhancement of mechanical and thermal properties of carbon fiber epoxy composite laminates reinforced with carbon nanotubes interlayer using electrospray deposition

Muhammad Razlan Zakaria[a,b], Hazizan Md Akil[c,*], Mohd Firdaus Omar[a,b], Muhammad Helmi Abdul Kudus[c], Fatin Nur Amirah Mohd Sabri[c], Mohd Mustafa Al Bakri Abdullah[a,b]

[a] Faculty of Chemical Engineering Technology, Universiti Malaysia Perlis (UniMAP), Perlis, Malaysia
[b] Geopolymer & Green Technology, Centre of Excellent (CEGeoGTech), Universiti Malaysia Perlis (UniMAP), Perlis, Malaysia
[c] School of Materials and Mineral Resources Engineering, Engineering Campus, Universiti Sains Malaysia, 14300 Nibong Tebal, Pulau Pinang, Malaysia

ARTICLE INFO

Keywords:
Carbon fiber
Carbon nanotube
Hybrid material
Epoxy composite laminates

ABSTRACT

Carbon nanotubes (CNTs) was successfully deposited onto the surface of woven carbon fiber (CF) using the electrospray deposition method to produce a woven hybrid CF-CNT. The effect of voltage and spray times on the morphology of the woven hybrid CF-CNT have been studied. The voltage and spray time is crucial towards achieving a homogeneous CNT coating on the woven CF surface. The epoxy composite laminated with optimized woven hybrid CF-CNT and woven CF without the deposited CNTs were then prepared, and its tensile and thermal properties subsequently determined. The results showed that the woven hybrid CF-CNT epoxy composite laminates tensile strength increased by ~21%, its tensile modulus increased by ~37%, its interlaminar shear strength increased by ~25%, and its thermal conductivity increased by ~35% relative to that of the woven CF epoxy composite laminates.

1. Introduction

Aircraft construction requires materials with properties such as high specific strength, low weight, fatigue-load-resistant, heat-resistant, crack-resistant, and corrosion-resistant [1]. These properties are common in carbon fiber (CF) epoxy composite laminates, which resulted in the increased interest in its use as a critical structural component in aircraft [2]. However, the mechanical properties of CF epoxy composite laminates are already well-established and has reached its limit to be further improved, especially in the transverse direction [3, 4], mostly due to the non-polar and inert surface of CF resulting in low wettability and adhesion between the CF and the polymer matrix at its interfacial region(s) [5, 6]. Previous works proposed hybridizing CF with nanoparticles such as carbon nanotubes (CNTs) to improve CF's surface interactions [7–9]. CNTs' extraordinary mechanical properties, such as high tensile strength and modulus, render it excellent for use as a reinforcing agent on CF's surface [10, 11]. The presence of CNT on the CF will also increase the latter's surface roughness and improve the interfacial adhesion between the CF and its matrix [12].

The first attempt at improving CF's surface was proposed by Downs and Baker (1991), where they grew carbon filaments on the CF's surface using the chemical vapor deposition (CVD) method [13]. A decade later, Thostenson et al. proposed the use of 304 stainless steel as a catalyst and acetylene as a carbon source to grow CNT on CF's surface via the CVD method at 660 °C [14]. CVD is currently a well-known method for hybridizing CF with CNT, and its product is known to have excellent mechanical properties in the transverse direction [15–17]. However, its mechanical properties in the longitudinal direction are low due to the degradation of the CF exposed to the high CVD processing temperatures [18]. In order to address this problem, researchers used ceramics such as silica and alumina to coat the CF's surface before growing the CNT on it to prevent its degradation at high processing temperatures [19]. Another drawback of the CVD method is difficulty in upgrading its production line to produce larger structures. CF can also be contaminated by the metal catalyst used to grow the CNTs.

Researchers proposed a method of flame synthesis to grow CNT on CF's surface, which require low processing temperature and a concise growth time relative to the CVD method with the express purpose of minimizing CF's degradation [20]. Oulanti et al. reported that the CNT growth time in the flame as being 0.3–0.6 s at 500 °C [21]. Researchers

* Corresponding author.
E-mail address: hazizan@usm.my (H. Md Akil).

https://doi.org/10.1016/j.jcomc.2020.100075
Received 13 August 2020; Received in revised form 22 September 2020; Accepted 7 November 2020

are also looking at alternative methods of hybridization at room temperatures, such as chemical functionalization and electrophoretic deposition (EPD) [22, 23]. Generally, chemical functionalization methods use oxidation treatment on the CF and CNT to introduce carbonyl, hydroxyl, carboxyl, or amine groups on the surface to form chemical bonds between CF and CNT. Meanwhile, the EPD method works based on the motion of the charged particle dispersed in liquid suspension to the opposite charge surface electrode under an applied electrical field. Since this method requires the introduction of oppositely-charged CF and CNT, the oxidation treatment uses strong acids such as nitric acid and sulfuric acid to functionalize the CF or CNT. Although these chemical functionalization and EPD were performed at room temperature, both approaches expose the CF and CNT to strong acids, which could damage them and degrade their subsequent mechanical properties. However, these methods have been reported to significantly improve the mechanical properties in the longitudinal direction [24, 25] due to the impressive 3-D network structure of the hybrid CF-CNT, which increases the fiber surface area and induces more mechanical interlocking between the fibers and the matrix.

Li et al. proposed hybridizing CF and CNT via the electrospray deposition (ESD) method to improve the mechanical properties in the transverse direction without sacrificing the mechanical properties in the longitudinal direction due to the degradation of CF by the processing condition [26]. They reported obtaining a homogeneous coating of CNT on the CF's surface, confirming that their approach did not result in any degradation to the CF [27], which can be attributed to the ESD method producing hybrid CF-CNT at room temperature and not exposing the CF and CNT to oxidation treatments. Epoxy resin was used as a binder to improve the adhesion between CF and CNT, which also eliminated the surface defects on the CF. Their approach also used high-electric fields to convert the suspension/liquid into uniform non-agglomerating nano or micro-droplets, which are suitable for producing micrometer-thin or thinner layers of spray and uniform coatings. Their approach has a few advantages, such as viability for large-scale production, simplicity, and cost-effectiveness.

This work analyzes the influence of voltage and spray time of the ESD method on the properties of the hybrid CF-CNT. This study utilizes the UV cure epoxy system as a binder in the CNT dispersion to replace the regular epoxy resin system used by previous researchers. The advantages of using the UV cure epoxy system is that the curing time can be decreased to mere seconds relative to the regular epoxy resin system, which takes invariably longer. Also, the woven hybrid CF-CNT epoxy composite laminates were prepared to elucidate the mechanical and thermal properties of the laminate when using vacuum-assisted resin transfer moulding (VARTM).

2. Experimental

2.1. Materials

Multi-walled CNT (external diameter of 20–30 nm, internal diameter of 5–10 nm, length of 10–30 μm) was purchased from Sky Spring Nanomaterials Inc., Houston, TX, USA (95% pure and used as-received). Woven CF (thickness of 0.3 mm) was purchased from Toray Industries Inc, Chuo-Ku, Tokyo. The fast cure and low viscosity UV epoxy adhesive of UV 367 was purchased from Penchem Technologies Sdn Bhd, Penang, Malaysia, and it requires at least 3 s to cure under UV light (320–380 nm) at 1000 mW/cm^2. The epoxy laminating systems EpoxAmite 100 resin and EpoxAmite 103 slow hardener were purchased from Smooth-On, Inc., Macungie, PA, USA. N-Methyl-2-Pyrrolidone (NMP) was purchased from Sigma-Aldrich, St. Louis, MO, USA, and used as received.

2.2. Preparation of hybrid CF-CNT via electrospray deposition

In order to prepare a CNT dispersion suitable for electrospraying deposition, 0.1 g of CNT was dispersed in 50 ml NMP using a sonicator (Q700, Qsonica, Melville, CT, USA) at a frequency of 50 kHz for ~10 h. 1 ml of UV 367 was added to the CNT dispersion, which improved the interaction between CNT and the woven CF. The woven CF was attached to a steel roller at a speed of 120 rpm and connected to the ground electrode in preparation for the electrospray deposition. A 20 ml syringe was then filled with the CNT dispersion and installed on a precision syringe pump (Model NE-1600, New Era Pump Systems Inc., Farmingdale, NY, USA). The precision syringe pump was placed on the adjustable plate, and it moves left-right at a speed of 0.5 rpm to ensure that the CNT spray encompasses the entirety of the woven CF. Then, a stainless-steel needle (inner diameter of 0.33 mm, length of 38 mm) with a flat end was fitted to the syringe and connected to high voltage precision power source (Model ES20P-20 W, Gamma High Voltage Research Inc., Ormond Beach, Fl, USA). The power source varies the applied voltage at a resolution of 0.1 kV and a maximum applied voltage of ~20 kV. Finally, a UV lamp was installed above the steel roller to ensure that the UV epoxy adhesive cures after the spray process. The electrospray deposition setup schematic diagram is shown in Fig. 1. A different applied voltage was used in this study, and CNT dispersion with a flow rate of 0.02 ml/h was used throughout the setup. The duration of the spray time varies at ~5–30 mins. The woven CF was left to dry for 24 h after the spraying deposition process. The spraying process was repeated on the opposite side of the woven CF. Table 1 shows the processing parameters used in this study. The Dino-Lite Edge digital microscope (Model: AM7115MZT) was used to image the electrospraying process while the CNT was deposited onto the CF's surface.

Table 1
Electrospray deposition processing parameter.

Samples	Voltage (kV)	Spray time (min)	Flow rate (ml/h)
Hybrid CF-CNT 6	6	15	0.02
Hybrid CF-CNT 10	10	15	0.02
Hybrid CF-CNT 15	15	15	0.02
Hybrid CF-CNT 20	20	15	0.02
Hybrid CF-CNT 15–5M	15	5	0.02
Hybrid CF-CNT 15–15M	15	15	0.02
Hybrid CF-CNT 15–30M	15	30	0.02

2.3. Characterization of the hybrid CF-CNT

A Field Emission Scanning Electron Micrograph (FESEM) (LEO SUPRA 35VP, Carl Zeiss, Germany) and high-resolution transmission electron microscope (HRTEM) (Model: Philip TECNAI 20) was used to image the surface morphology of the woven CF and woven hybrid CF-CNT. The surface of the woven CF and woven hybrid CF-CNT was coated with a thin layer of gold (Au) to increase its conductance for imaging in the FESEM.

The woven hybrid CF-CNT epoxy composite laminates were prepared using the VARTM process, resulting in a sample measuring (300 × 210 × 2.5) mm. The optimization of the voltage and deposition time was based on the morphological assessment of the samples as opposed to the mechanical properties of the composites due to limitations associated with the number of specimens and resources. The optimized voltage and processing time was subsequently used to produce uniform CNT coating on the woven hybrid CF-CNT. A rubber gasket was placed around the perimeter of the mold halves to seal it properly. In the mould's cavity, eight layers of woven hybrid CF-CNT, produced based on the optimized applied voltage and spray time, were stacked to form a plate with a thickness of 2.5 mm. A vacuum was applied to the mold to create the pressure gradient needed to infiltrate the epoxy suspension into the preform. There was no gap between the edge of the mold and the woven hybrid CF-CNT preform, which prevents the flow path outside the preform from reflowing into the vacuum port. EpoxAmite 100 resin and EpoxAmite 103 slow hardener were mixed at a 100:27 mass ratio and drawn into the mold via a tube. The epoxy suspension flows

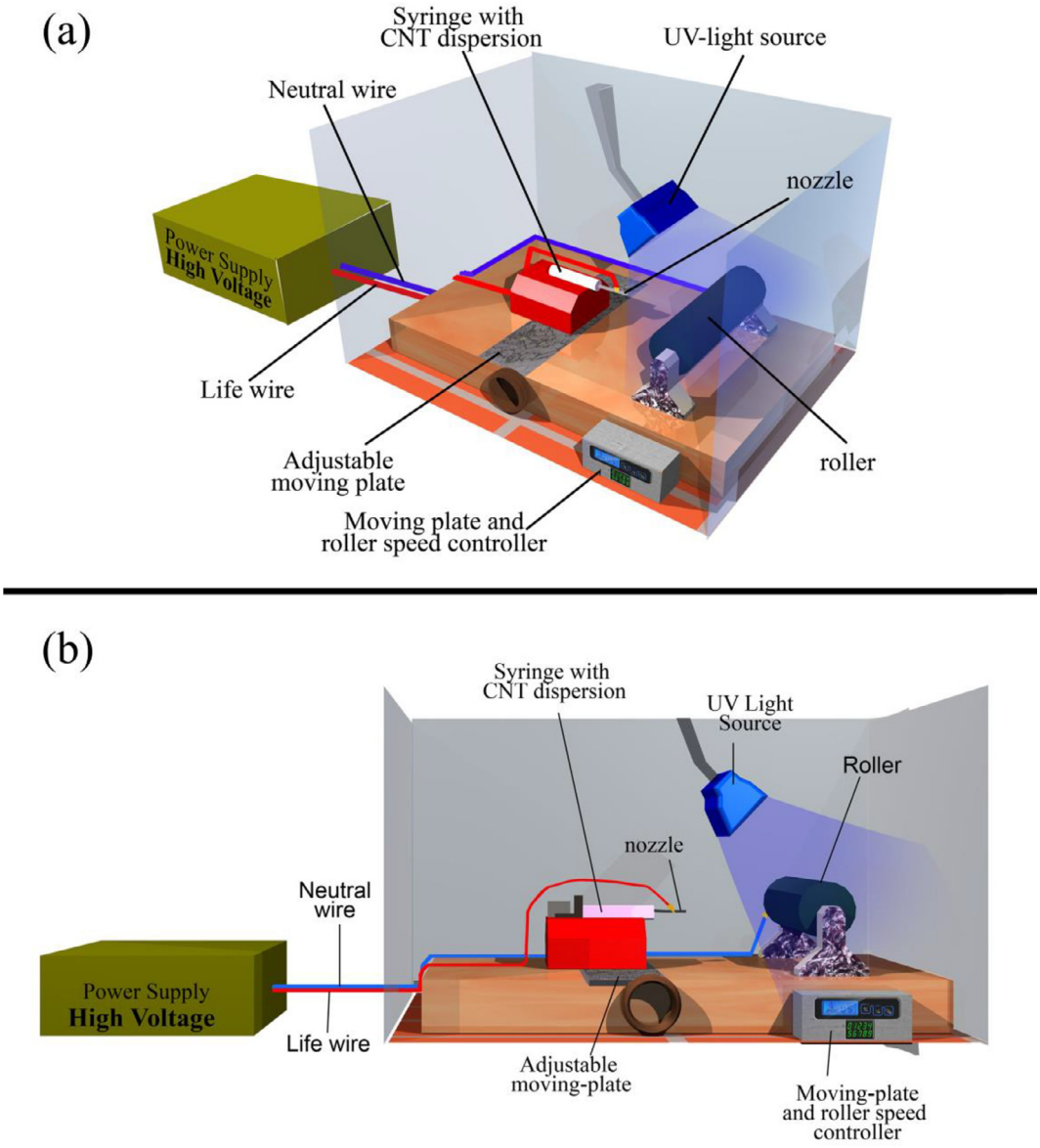

Fig. 1. Schematic diagram of electrospray setup.

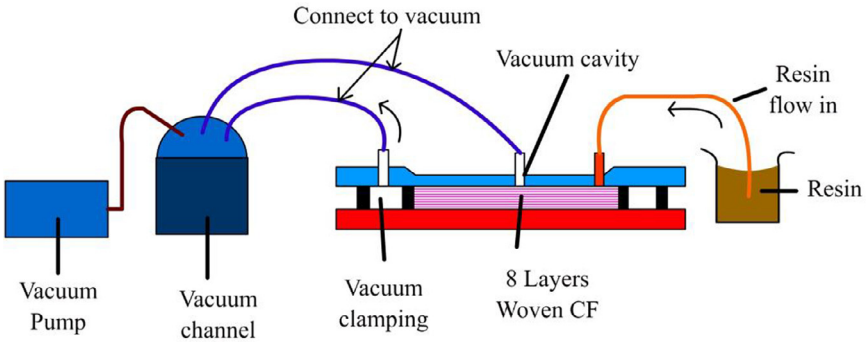

Fig. 2. Schematic diagram of the VARTM setup.

in the direction of the thickness across the fiber layers, and the injection was discontinued as soon as the epoxy suspension reached the vent at the top, but the vacuum state was maintained (75 cm Hg). After the epoxy suspension cured, the vacuum was discontinued, and the part of the woven hybrid CF-CNT epoxy composite laminate was de-moulded. Fig. 2 shows the experimental setup for the VARTM process. For comparison purposes, a woven CF epoxy composite laminates were prepared using the same method. Table 2 tabulates the samples' characteristics.

2.5. Characterization of woven hybrid CF-CNT epoxy composite laminates

The tensile properties of CF/Epoxy and CF-CNT/Epoxy were quantified using a universal testing machine (Model: 5982, Instron, USA) and carried out as per the ASTM D3039. The tensile test samples were cut from the CF/Epoxy and CF-CNT/Epoxy panels at measurements of 250 mm (length) x 25 mm (width) x 2.5 mm (thickness). A crosshead speed of 2.0 mm/min was used, and for each sample, at least five were

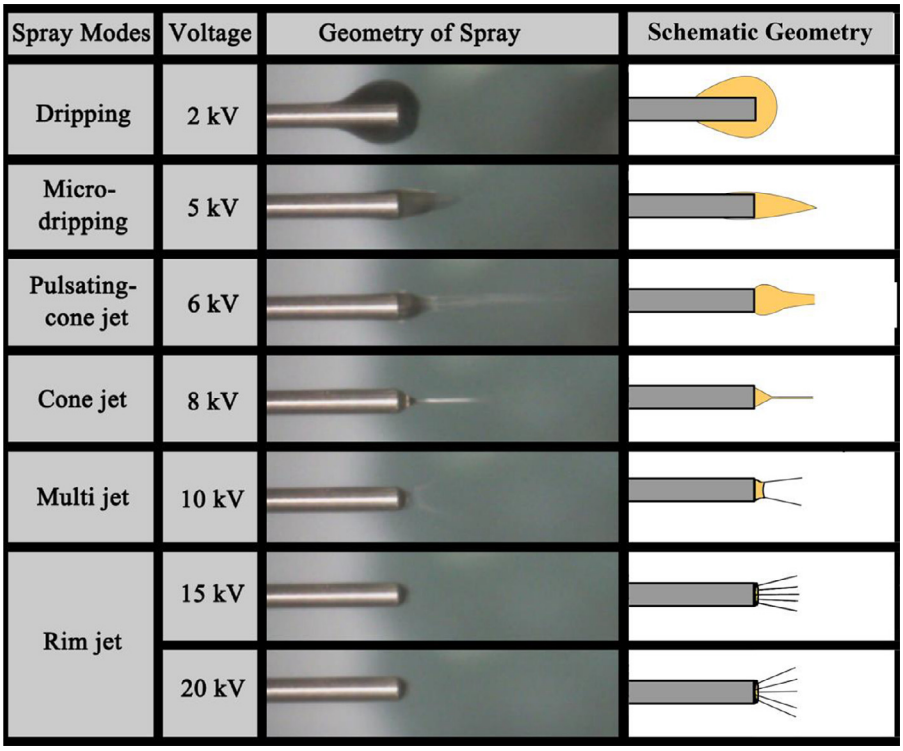

Fig. 3. Electrospray modes at a different applied voltage of 2 – 20 kV.

Table 2
Descriptions of the samples.

Samples	Descriptions
CF/Epoxy	Epoxy reinforced with 8 layers of woven CF
CF-CNT/Epoxy	Epoxy reinforced with 8 layers of woven hybrid CF-CNT

tested to ensure the results' reliability. The fracture surface of the tensile specimens was coated with a thin layer of Au after the test and imaged using the FESEM. The density of the CF/Epoxy and CF-CNT/Epoxy were determined using a density balance (Model: Precissa XT 220A) with methanol as its liquid medium. The interlaminar shear strength (ILSS) of the composite laminates were quantified using the short beam strength (SBS) test as per the ASTM standard D2344. The samples were cut from the CF/Epoxy and CF-CNT/Epoxy panel, measuring 20 mm (length), 5 mm (width) and 2.5 mm (thickness). The SBS test was conducted with a test span of 10 mm at a crosshead speed of 1 mm/min. At least five specimens were tested for each case to ensure the reliability of the test results. The thermal conductivity of the CF/Epoxy and CF-CNT/Epoxy were determined using a Hot Disk Thermal Constants Analyzer (Model: TPS 2500S). The Hot Disk Thermal Constants Analyzer sensor was placed between two identical samples measuring 30 mm x 30 mm x 2.5 mm.

3. Results and discussion

It is well-established that the processing conditions significantly influence the electrospray modes during the electrospraying process. The electrospraying mode is categorised via the meniscus geometry of the spray at the end of the nozzle tip. Fig. 3 shows the electrospray modes at applied voltages of ~2 - 20 kV using a digital microscope under similar processing conditions of the CNT dispersion, nozzle sizes, and flow rates. In this experiment, electrospray modes such as dripping, micro-dripping, pulsating-cone jet, cone jet, multi-jet and rim jet are characterized by the applied voltages. In the dripping mode, the CNT dispersion was ejected as a sizeable spherical droplet from the capillary nozzle toward the collector. The spray current in this dripping mode is independent of the voltage within 0 - 2 kV. The micro-dripping mode is observed as the applied voltage increases to 5 kV. In this mode, the droplet size becomes smaller, and its dripping frequency increases. Due to the large size of the droplet in the first two modes and inadequate solvent evaporation within the droplet before it arrives at the collector, both modes are unsuitable for producing uniform CNT deposition.

Further increasing the applied voltage to ~6 kV resulted in the formation of the pulsating-cone jet. In this mode, the diameter of the jet decreases and the jet is emitted intermittently, consisting of phases such as liquid accumulation, cone formation, jet ejection, and relaxation phases [28]. Also, the diameter of the jet during this mode varies depending on the phases and distribution of the droplet size not monodispersing. As the applied voltage is increased to ~8 kV, its meniscus is elongated, and a stable cone jet is observed. During this mode, the diameter of the jet decreases significantly, forming a cone jet with a thin jet originating from its apex. When the applied voltage is further increased, a multi-jet can be seen at a voltage of 10 kV while a rim jet can be seen when the voltage exceeds ~15 kV. In the rim jet mode, it can be seen that the meniscus becomes flat and fine liquid jets are ejected from the capillary nozzle. Also, the number of emission points increased with increasing voltage because the higher electrical energy facilitates disruption of the meniscus at more sites, leading to more emission points [29].

Fig. 4 shows the SEM images of the as-received woven CF. Based on the images, the smooth surface of the woven CF with grooves running along the longitudinal direction is evident. Fig. 5 shows the SEM images of the hybrid CF-CNT produced as a function of varying the voltage. The most critical parameter to consider in order to achieve a homogeneous CNT coating on the woven CF is the optimization of the electrospraying voltage. The poor distribution of the CNT on the woven CF surface is evident at a voltage of 6 kV. There are some areas of the woven CF surface that are not coated by CNT, and CNT accumulation regions are also evident in the images, both of which can be attributed to the large droplets being present in the pulsating-cone jet mode. Increasing the voltage to 10 kV, the distribution of CNT on the woven CF surface improved. Although there are accumulations of CNT, the CNT is well distributed and covers the entirety of the woven CF surface. When the voltage is in-

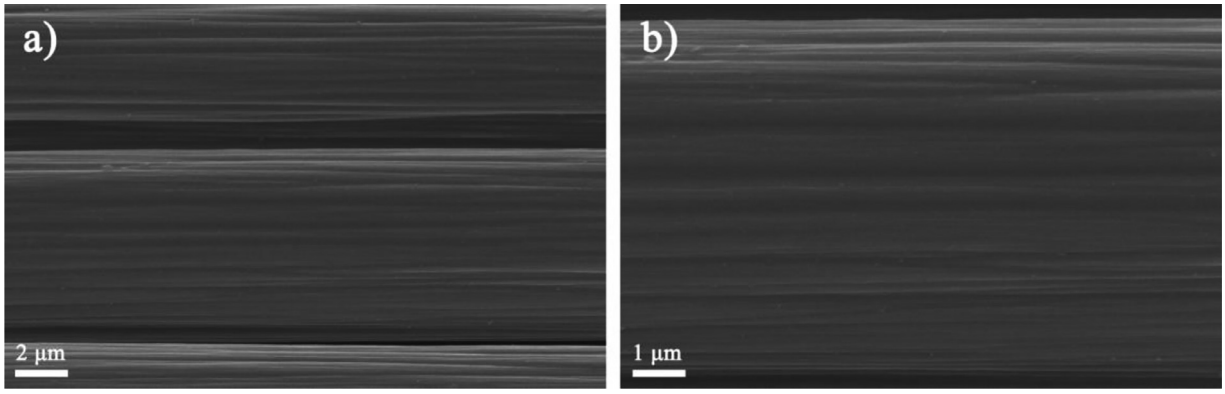

Fig. 4. SEM images of CF with magnification of (a) 5000X and (b) 10000X.

creased to ~15 kV, the CNT is seen to be homogeneously distributed and fully covering the woven CF surface, which can be attributed to the increasing number of emission points in the rim jet mode, resulting in an adequate deposition that prevents the accumulation of the CNT. At a voltage of ~20 kV, although some region of woven CF was uncoated by CNT, the CNT is not accumulated on the woven CF surface.

Further increasing the voltage leads to an increase in the spray range distance and width. Increasing the voltage to higher levels will lead to wastage of CNTs and safety problems. Based on the results, it can be surmised that the optimal voltage to produce a uniform CNT coating on woven CF surface is ~15 kV.

Fig. 6 shows the SEM images of hybrid CF-CNT produced as a function of the deposition time at ~15 kV. Based on the images, the number of CNTs on woven CF surface increase with increasing deposition time. At a deposition time of 5 mins, only a small amount of CNT is deposited on the woven CF surface, and large gaps between each CNT fiber is evident. Also, at 5 mins deposition time, the grooves running along the longitudinal direction on the woven CF surface is evident. The woven CF is fully coated with CNT when the deposition time was increased to 15 min. The woven CF is coated with a thin layer of CNT, and it can still be seen the woven CF surface. However, further increasing the deposition time to 30 mins resulted in a thick layer of CNT deposited onto the woven CF surface. The thick layer of the CNT entirely covered the surface of the woven CF, and it could no longer be seen the surface of the woven CF. Also, large quantities of deposited CNT forced it into contact with each other at the CF's surface, which also fills the gap present between the CFs.

The CF/Epoxy and CF-CNT/Epoxy were tensile tested to determine the reinforcement effects of the woven CF and woven hybrid CF-CNT on the tensile properties of the resulting epoxy composite laminates. Fig. 7 shows the typical stress-strain curves obtained from the tensile tests of the CF/Epoxy and CF-CNT/Epoxy. It can be seen based on the magnitude of the recorded strain that the composite is significantly brittle, and the addition and presence of the CNTs further increased the brittleness of the composite while simultaneously making it more robust, as per its higher failure stress. Fig. 8a and b show the average tensile strength and tensile modulus obtained from the stress-strain curve. The CF-CNT/Epoxy has higher tensile strength and tensile modulus relative to the CF/Epoxy. The CF-CNT/Epoxy has the highest tensile strength at 641 MPa, which is 21% higher than that of CF/Epoxy. Few factors contribute to the improvement of the tensile strength of epoxy composite laminates, such as fiber or particle distribution in the matrix, interfacial adhesion, and the strength of the matrix material [30]. The higher tensile strength of CF-CNT/Epoxy relative to that of the CF/Epoxy can be attributed to the presence of the CNTs, which changes the interfacial behavior. CF has a non-polar surface and inert structure, which induces weak interfacial adhesion between the woven CF and its matrix. The deposition of the CNTs on the woven CF surface resulted in decreased total CF/matrix interfacial area and increased CNT/matrix interfacial area. The abovementioned observation has been reported elsewhere [31], where there are two reinforcing elements involved in the CF-CNT/Epoxy system, leading to two interfaces resembling that of the CF/matrix and CNT/matrix. Also, the presence of CNT on the woven CF surface increases the surface roughness of the woven CF, allowing it to carry loads, which improves the stress transfer between the woven CF and epoxy matrix. Twists and kinks in the CNT structure create mechanical interlocks between the CNT and epoxy matrix [32] and the extraordinary mechanical properties of the CNTs were expected to improve the tensile strength of the CF-CNT/Epoxy.

The tensile modulus of the CF/Epoxy and CF-CNT/Epoxy show similar increasing trends as that of the tensile strength. The CF-CNT/Epoxy reported the highest tensile modulus, with an increase of up to ~32.4 GPa, corresponding to an increase of ~37% relative to that of the CF/Epoxy. The higher tensile modulus of the CF-CNT/Epoxy is due to the presence of the CNTs on the CF's surface, which improves the tensile modulus by restricting the mobility of the polymer chain under load [33]. The presence of CNTs also increased the cross-linking ratio and blocked the molecular motions of the epoxy matrix [34]. The high surface area, high modulus, and the strength of the CNT also resulted in improved tensile modulus. Similar increasing trends of tensile strength and tensile modulus are consistent with previous studies reported by other researchers. Mei et al. reported significant improvements in tensile strength and tensile modulus of epoxy composites by depositing CNT on the CF surface using the electrophoretic method [35]. In their work, the tensile strength and tensile modulus improved by ~36% and ~4% compared to CF without CNT, respectively. Hung et al. introduced CNTs on CF's surface using the CVD method, and the resulting tensile strength and tensile modulus of the epoxy composites improved by ~9% and ~4%, respectively, compared to CFs without CNT [31]. Davis et al. used amine functionalization to attach CNT on the CF surface, and reported improvement to the tensile strength and tensile modulus of the epoxy composites by ~10% and ~19%, respectively [36]. The increase in tensile properties is in agreement with Maoseri et al. [34, 37], Hung et al. [31] and Rahmanian et al. [38]. Based on the previous works, depositing CNTs on CF's surface improve the tensile strength and tensile modulus of epoxy composites. Despite the higher tensile strength and tensile modulus of the CF-CNT/Epoxy, the fracture strain of the CF-CNT/Epoxy is slightly lower than that of the CF/Epoxy without the CNT. The presence of the CNTs enhanced load bearing capacity, as per the higher tensile stress at failure, but it also decreases the magnitude of extensibility due to the increased rigidity in its internal structure.

The fracture surface of the tensile test specimens of CF/Epoxy and CF-CNT/Epoxy were examined using SEM to elucidate their fracture behaviours, as per Fig. 9. It can be seen that both samples failed in the brittle mode, as per its sudden failures. There is also the absence of necking on the fracture surface as per the SEM images of the CF structure, and

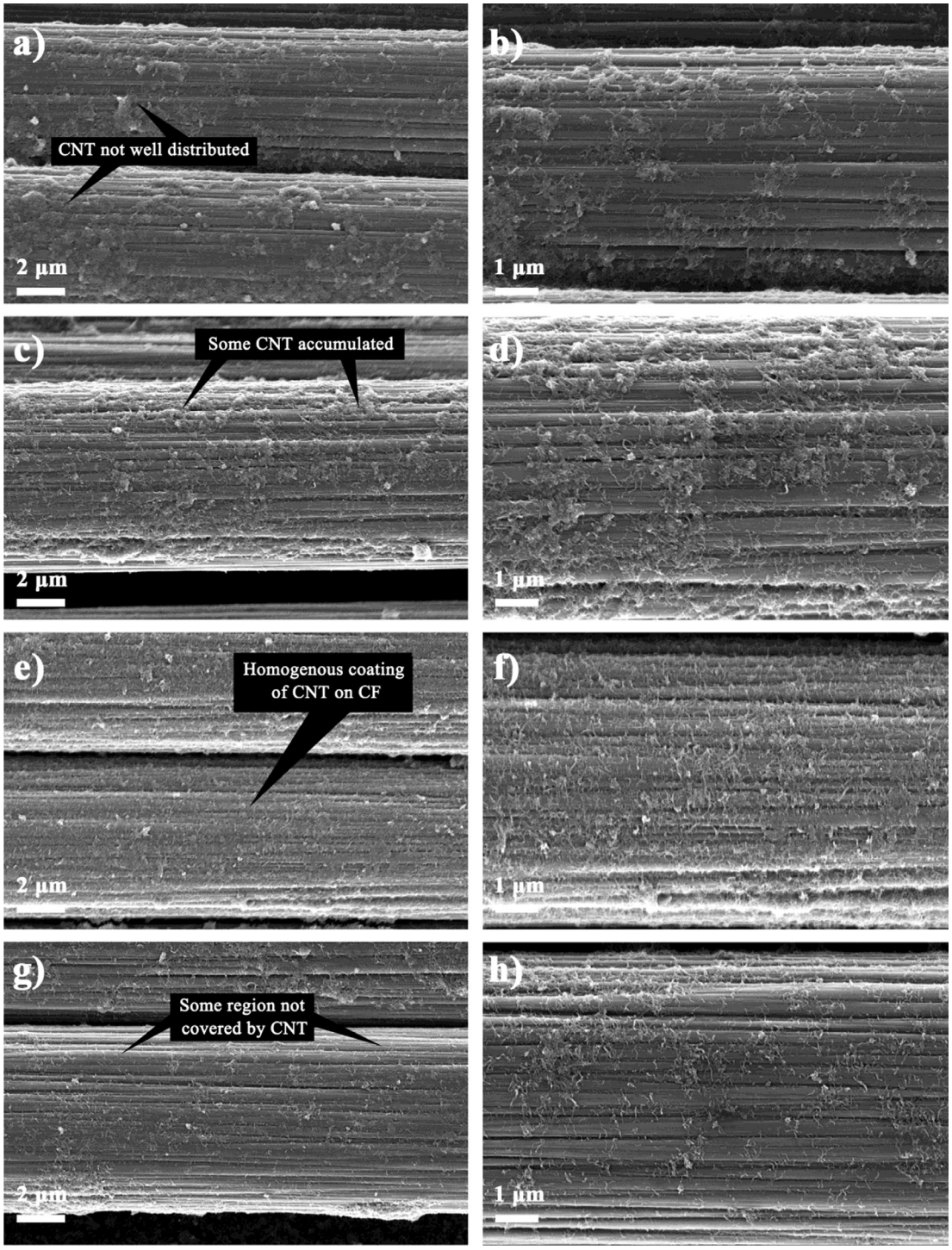

Fig. 5. SEM images of hybrid CF-CNT produced as a function of varying voltage (a-b) 6 kV, (c-d) 10 kV, (e-f) 15 kV and (g-h) 20 kV.

the surface of the CF failure is irregular, serrated, and non-planar. In the case of the CF/Epoxy in Fig. 9 (a, c and e), there are minimal signs of interaction at the CF/epoxy matrix interface, which is evident due to the smooth CF surface with only a few residual epoxy resins on the CF's surface. The crenulations on the CF's surface can also be seen. In the case of the CF-CNT/Epoxy in Fig. 9 (b, d and f), the deposited CNT on the CF surface completely altered the interfacial behavior, resulting in a different fracture morphology. The relatively rough surface on the hybrid CF-CNT surface is evident. The presence of epoxy resin on the hybrid CF-CNT surface is indicative of excellent interfacial interactions between the hybrid CF-CNT and the epoxy matrix. Additionally, some of the CNT remained unperturbed on the CF's surface post-fracture, which means that the ESD method is capable of firmly attaching the CNTs onto the CF's surface when using the UV-cured epoxy as a binder. The strong bonds between the CNTs and CF are crucial towards ensuring robust interlocks between the CNTs and the epoxy matrix.

The increase in the tensile strength at failure in the case of the CF-CNT/Epoxy can be attributed to several mechanisms [31], with 3 possibilities for the hybrid CF-CNT to fracture/pullout from the epoxy matrix, as can be seen in Fig. 10. In type 1 fracture, the CNTs remains firmly attached to the CF, and the CNTs along the CF are de-bonded from the epoxy matrix, which can be attributed to the strong adhesion between

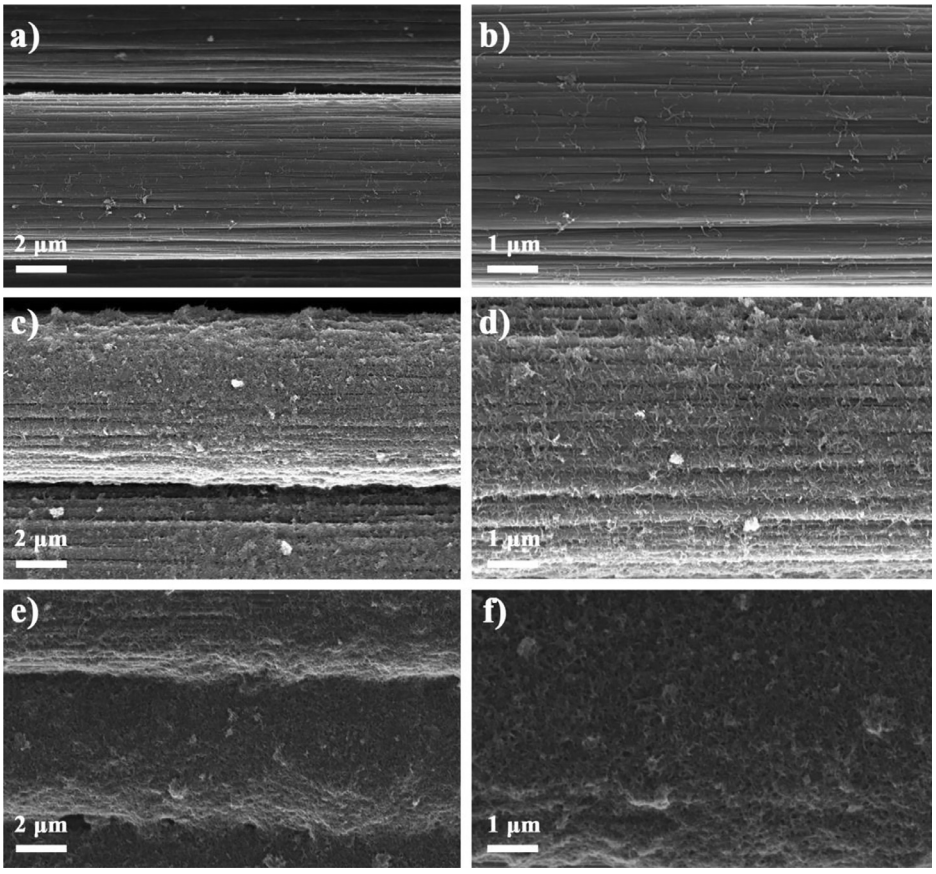

Fig. 6. SEM images of hybrid CF-CNT produced as a function of deposition time at 15 kV (a-b) 5 min, (c-d) 15 min and (e-f) 30 min.

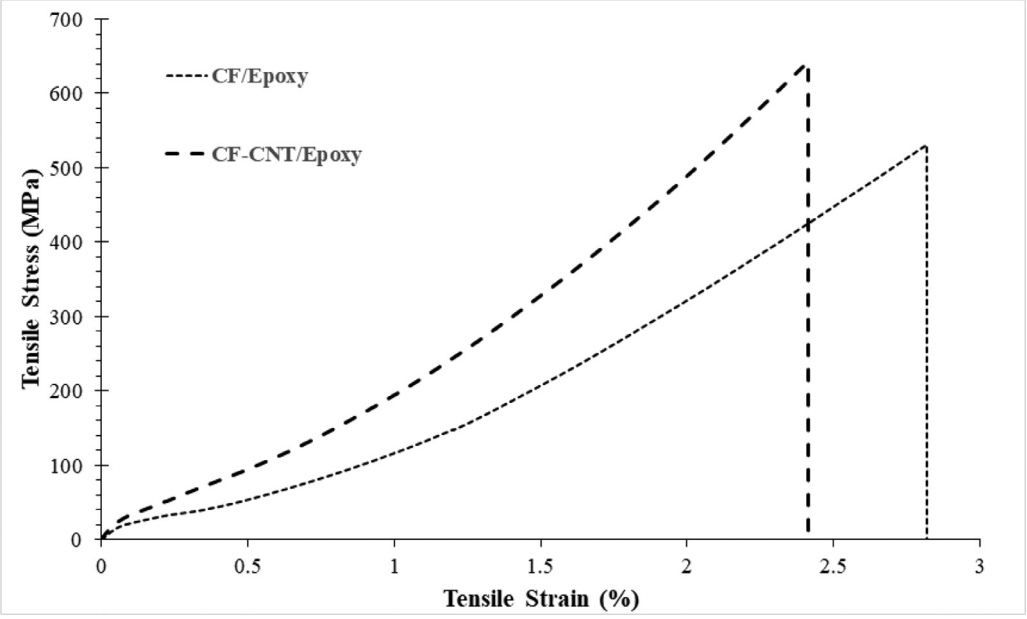

Fig. 7. Tensile stress-strain curves of CF/Epoxy and CF-CNT/Epoxy.

the CNTs and CF. In type 2 fracture, the CNTs is detached from the CF, and the detached CNTs remains buried within the epoxy matrix, which occurs in the region where the CNT and CF are weakly bonded. In type 3 fracture, the CNT is fragmented, with half of the CNT remaining attached to the CF while the other half remains buried within the epoxy matrix. Based on the SEM image of the fracture surface, it is clear that the type 1 fracture is dominant.

Table 3 shows the densities, specific tensile strengths, and specific tensile moduli of the CF/Epoxy and CF-CNT/Epoxy. Based on the results, it can be seen that the density of the CF-CNT/Epoxy is higher compared to CF/Epoxy due to the CNTs deposition on the CF's surface. The specific tensile strength and specific tensile modulus are required to take into account the epoxy composite laminates density. Although the CF-CNT/Epoxy has a slightly higher density compared to CF/Epoxy, it has a specific tensile strength and specific tensile modulus higher than that of the CF/Epoxy.

The interfacial adhesion between woven CF and epoxy matrix was evaluated using via its ILSS. Fig. 11 shows the ILSS of the CF/Epoxy

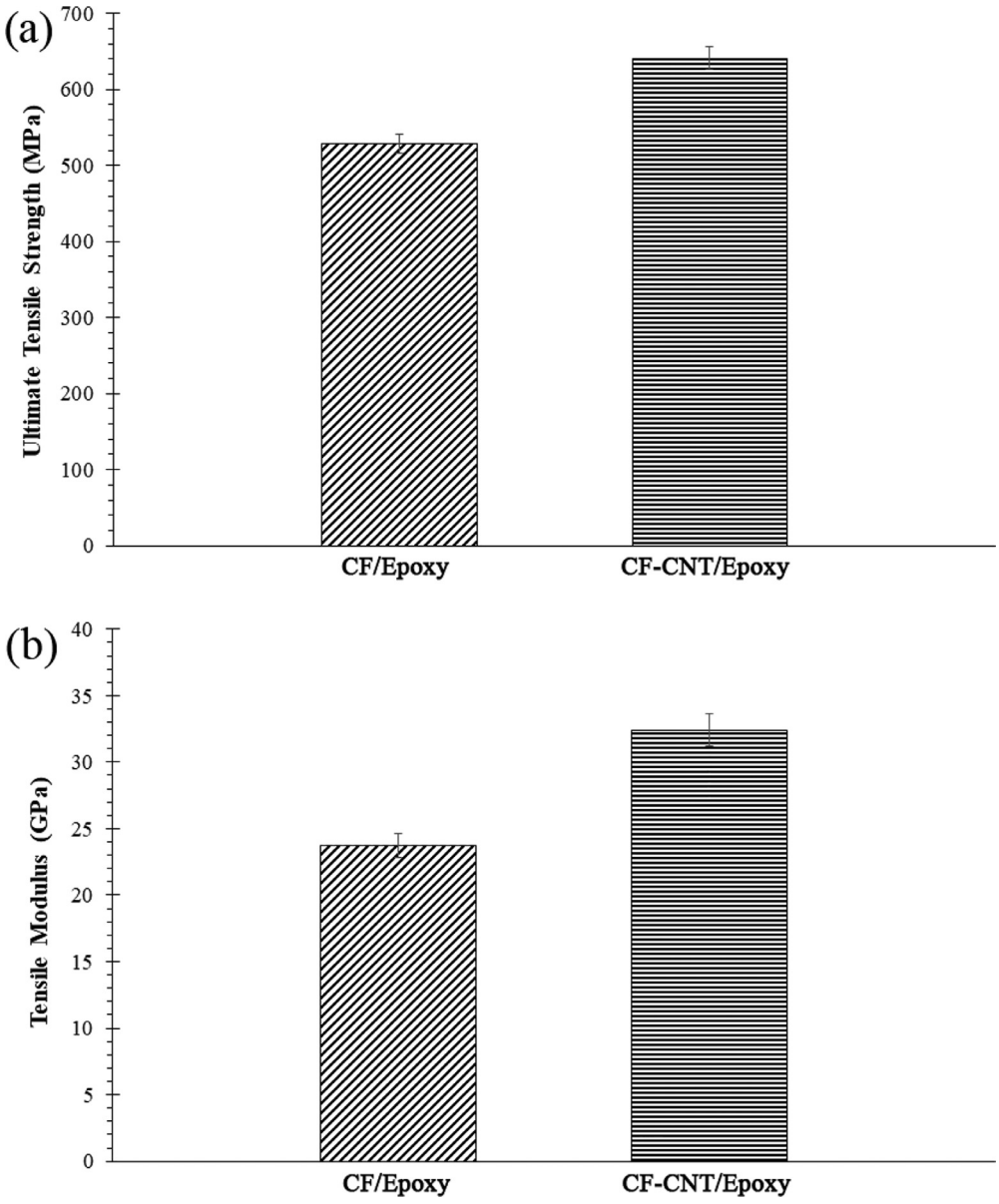

Fig. 8. Tensile properties of the CF/Epoxy and CF-CNT/Epoxy (a) ultimate tensile strength and (b) tensile modulus.

Table 3
Density, specific tensile strength and specific tensile modulus of CF/Epoxy and CF-CNT/Epoxy.

Properties	CF/Epoxy	CF-CNT/Epoxy
Density (g/cm^3)	1.340	1.373
Specific tensile strength (MPa/(g/cm^3))	395	467
Specific tensile modulus (GPa/(g/cm^3))	17.7	23.6

and CF-CNT/Epoxy. The result shows that the CF-CNT/Epoxy has the highest ILSS, with an increase of ~48.9 MPa, corresponding to a 25% increase relative to that of CF/Epoxy. It can be surmised that the woven CF with deposited-CNT affect the properties of the composite interfacial adhesion. These results are indicative of the fact that the CNTs deposited on the woven CF improved the interfacial adhesion of the CF-CNT/Epoxy by increasing the surface roughness of the woven CF, which induced stronger interfacial mechanical interlocking between the fiber and the matrix. Also, the reinforcement effect induced by the CNT in the direction perpendicular to the woven CF axis prevents interlaminar sliding and de-bonding. This finding is consistent with earlier reports of enhanced CF and epoxy matrix interfacial bonding by depositing CNT on CF's surface. Zhao et al. reported improvements of 15% in the ILSS of the epoxy composites by depositing CNTs on the CF's surface using the electrophoretic deposition method [24]. Garcia et al. used the CVD method to grow the CNT on the CF's surface and reported a ~69% improvement in the ILSS of epoxy composites [39]. Li et al. bound hydroxyl-functionalized CNT to carboxylic acid-functionalized CF, and reported a ~13% increase in the ILSS of epoxy composites [40]. Although CNTs represent a tiny overall volume fraction of the composite, it is nevertheless capable of modifying the macroscopic mechanical properties of the composite.

Fig. 12 shows the thermal conductivity of the CF/Epoxy and CF-CNT/Epoxy. It can be seen that the CF-CNT/Epoxy had higher thermal conductivity relative to CF/Epoxy. The CF-CNT/Epoxy has a thermal conductivity of 0.97 W/mK, which corresponds to an increase of ~35% relative to that of the CF/Epoxy. The significant increase in thermal conductivity of the CF-CNT/Epoxy is due to the deposition of the CNTs on the woven CF's surface. The CNTs on the woven CF's surface served as a thermal bridge between the layers of woven CF laminates by forming thermal chains, which enhances the heat flow in the epoxy composite laminates. In the CF/Epoxy system, the direction of the phonon travel in the epoxy composite laminates depended on the one-dimensional (1D)

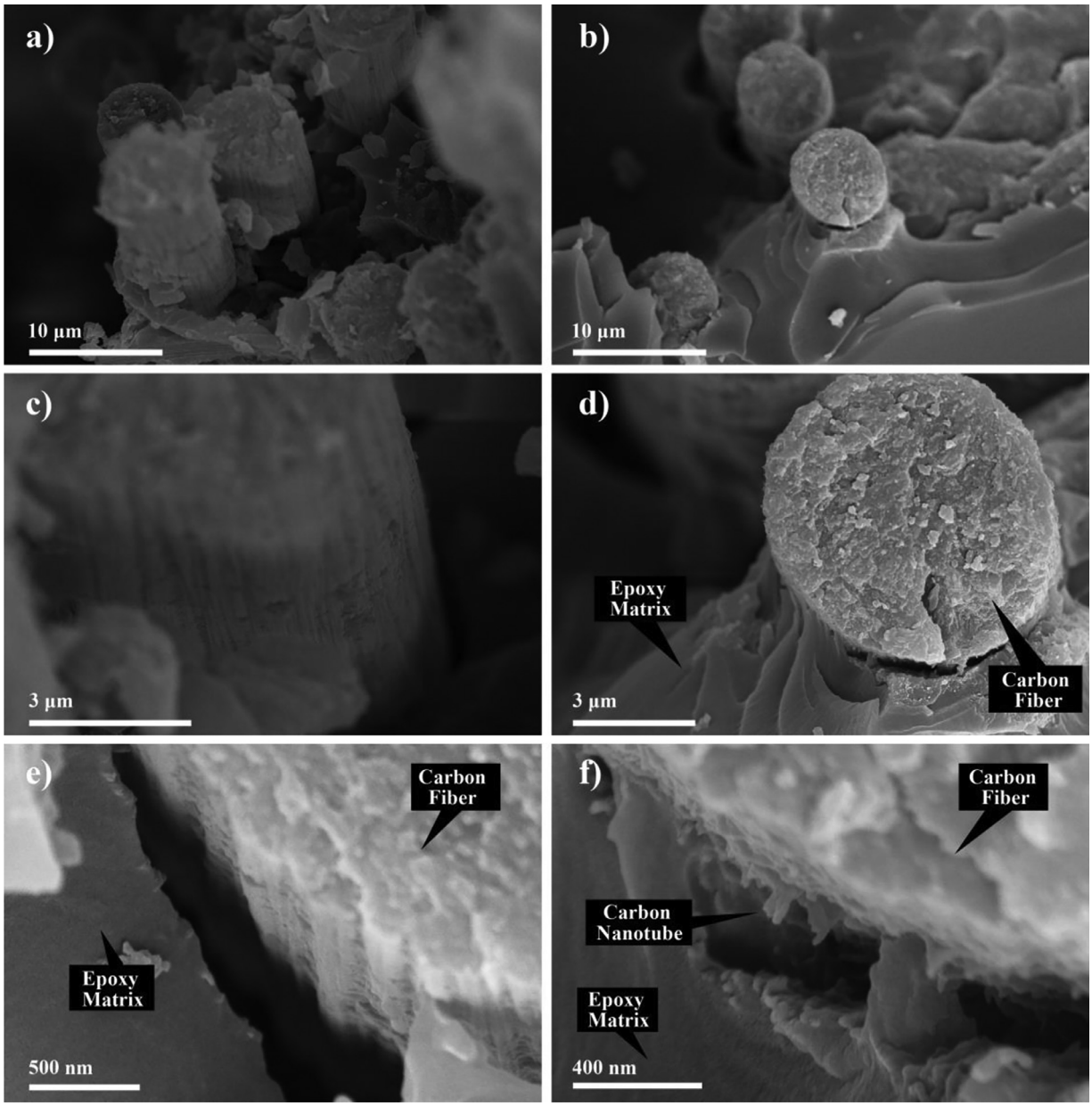

Fig. 9. SEM images of the fracture surfaces of (a, c and e) CF/Epoxy and (b, d and f) CF-CNT/Epoxy.

structure of the CF. The 1-D structure of the CF limit phonon travels on the epoxy composite laminates.

Meanwhile, in the CF-CNT/Epoxy system, the hybridization of the 1-D structure of CF and 1-D structure of the CNTs formed a 3-D structure of hybrid CF-CNT, which resulted in a network of thermal conductor that allows phonon travel in the epoxy composite laminates. Thus, the hierarchical 3-D structure of hybrid CF-CNT helped the phonon travel efficiently on epoxy composite laminates. Also, the large specific surface area and extraordinary thermal conductivity of CNT, which has a thermal conductivity up to 3000 W/mK, are also beneficial for enhancing thermal conductivity of CF-CNT/Epoxy. Other researchers have also reported increasing thermal conductivity by depositing CNT on CF in polymer composites [41]. Wang et al. posited that depositing CNT on CF increased the surface roughness of CF and increase the crystallinity of the CF's surface that has a positive effect on improving the thermal conductivity of polymer composites [42].

5. Conclusion

This study confirmed that a woven hybrid CF-CNT could be produced using the electrospray deposition method. The final morphology of the woven hybrid CF-CNT was found to be strongly influenced by voltage and spray time. Based on the experimental findings, it can be concluded that the optimal voltage and spray time for producing a homogeneous and even CNT coating on woven CF's surface is ~15 kV and 15 mins, respectively. The woven hybrid CF-CNT epoxy composite laminates have superior tensile and thermal properties relative to that of the woven CF epoxy composite laminates. The enhancement in tensile strength, tensile modulus, ILSS, and thermal conductivity of the woven hybrid CF-CNT epoxy composite laminates are ~21%, ~37%, ~25%, and ~35%, respectively, which can be attributed to the presence of the CNTs on the woven CF surface forming a 3-D network structure that significantly improved the load and thermal transfer capabilities in the epoxy composite laminates.

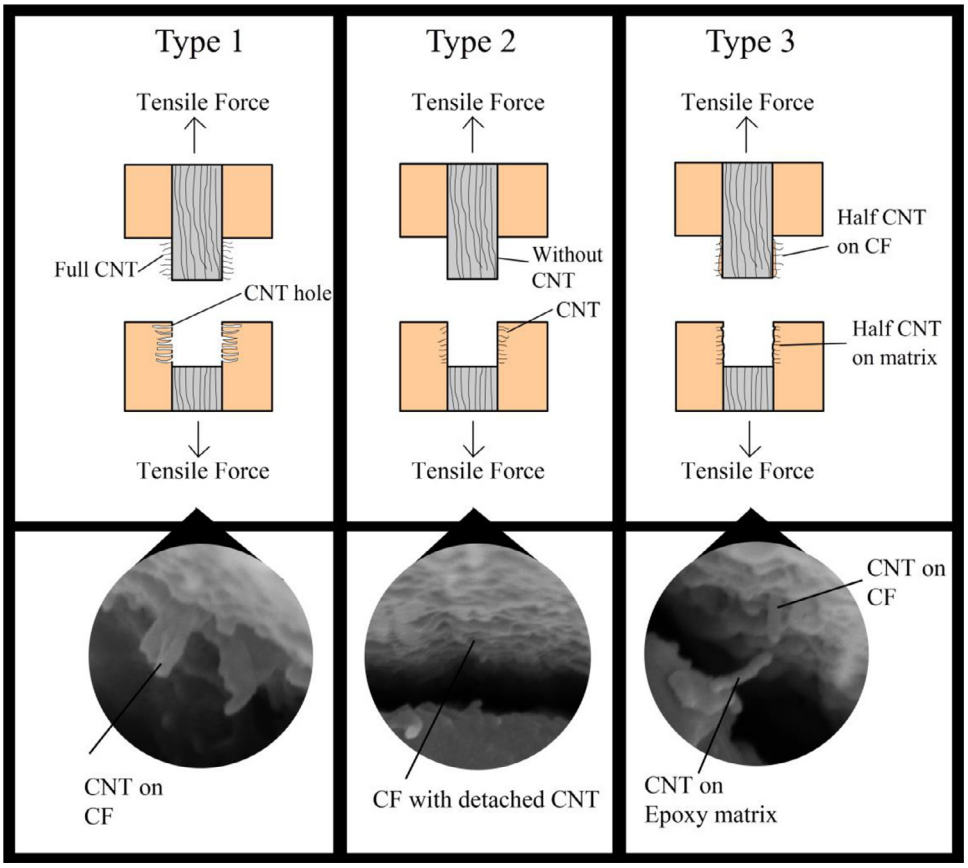

Fig. 10. Schematic diagram of hybrid CF-CNT fracture or pullout from the epoxy matrix.

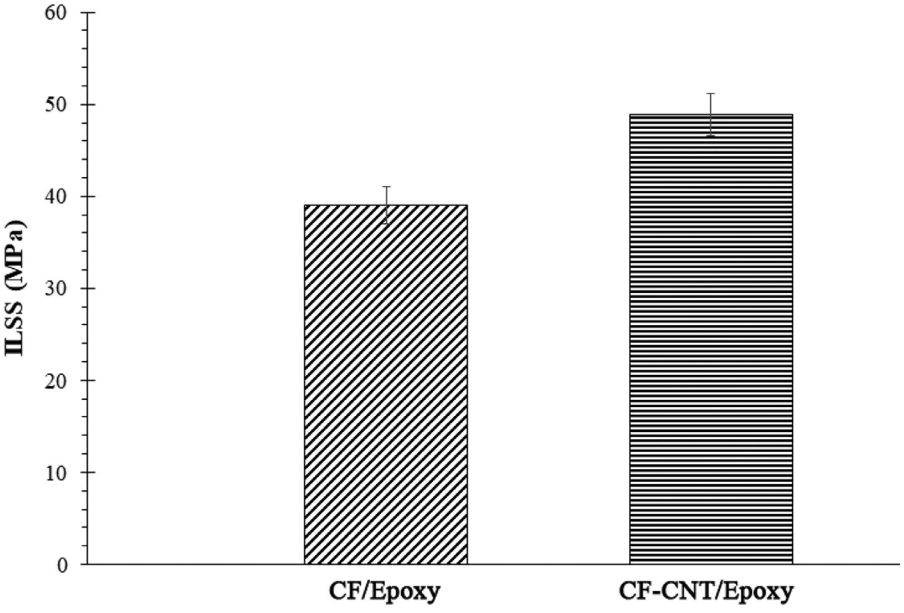

Fig. 11. ILSS of the CF/Epoxy and CF-CNT/Epoxy.

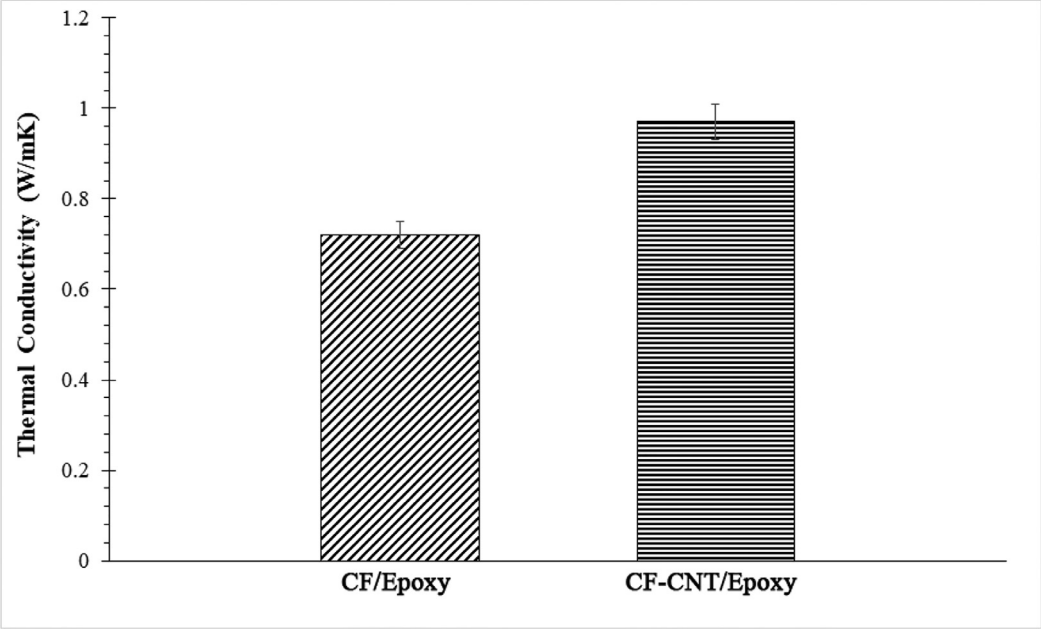

Fig. 12. Thermal conductivity of CF/Epoxy and CF-CNT/Epoxy.

Declaration of Competing Interests

None.

Acknowledgement

The authors would like to acknowledge Universiti Sains Malaysia (USM) RUI 1001/PBAHAN/8014047 for sponsoring and providing financial assistance during this research work and Universiti Malaysia Perlis for sponsoring postdoctoral fellowship.

References

[1] C. Soutis, Fibre reinforced composites in aircraft construction, Progr. Aerosp. Sci. 41 (2) (2005) 143–151.
[2] S.J. Lewis, The use of carbon fibre composites on military aircraft, Compos. Manuf. 5 (2) (1994) 95–103.
[3] A. Boroujeni, M. Tehrani, A. Nelson, M Al-Haik, Hybrid carbon nanotube–carbon fiber composites with improved in-plane mechanical properties, Compos. Part B: Eng. 66 (2014) 475–483.
[4] S. Karmakov, F. Cepero-Mejías, J.L Curiel-Sosa, Numerical analysis of the delamination in CFRP laminates: VCCT and XFEM assessment, Compos. Part C: Open Access 2 (2020) 100014.
[5] L. Zhang, N. De Greef, G. Kalinka, B. Van Bilzen, J.-.P. Locquet, I. Verpoest, et al., Carbon nanotube-grafted carbon fiber polymer composites: damage characterization on the micro-scale, Compos. Part B: Eng. 126 (2017) 202–210.
[6] X. Li, M. Saeedifar, R. Benedictus, D Zarouchas, Damage accumulation analysis of cfrp cross-ply laminates under different tensile loading rates, Compos. Part C: Open Access 1 (2020) 100005.
[7] B. Wang, Q. Fu, T. Yin, H. Li, L. Qi, Y Fu, Grafting CNTs on carbon fabrics with enhanced mechanical and thermal properties for tribological applications of carbon fabrics/phenolic composites, Carbon N Y (2018).
[8] A.Y. Boroujeni, M. Al-Haik, Carbon nanotube – Carbon fiber reinforced polymer composites with extended fatigue life, Compos. Part B: Eng. 164 (2019) 537–545.
[9] W. Zhang, X. Deng, G. Sui, X Yang, Improving interfacial and mechanical properties of carbon nanotube-sized carbon fiber/epoxy composites, Carbon N Y 145 (2019) 629–639.
[10] M.R. Zakaria, M.H. Abdul Kudus, H. Md. Akil, M.Z Mohd Thirmizir, Comparative study of graphene nanoparticle and multiwall carbon nanotube filled epoxy nanocomposites based on mechanical, thermal and dielectric properties, Compos. Part B: Eng. 119 (2017) 57–66.
[11] V.K. Patle, R. Kumar, A. Sharma, N. Dwivedi, D. Muchhala, A. Chaudhary, et al., Three dimension phenolic resin derived carbon-CNTs hybrid foam for fire retardant and effective electromagnetic interference shielding, Compos. Part C: Open Access 2 (2020) 100020.
[12] S. Zhu, C.-.H. Su, S. Lehoczky, I. Muntele, D Ila, Carbon nanotube growth on carbon fibers, Diam. Relat. Mater. 12 (10–11) (2003) 1825–1828.
[13] W. Downs, R Baker, Novel carbon fiber-carbon filament structures, Carbon N Y 29 (8) (1991) 1173–1179.
[14] E. Thostenson, W. Li, D. Wang, Z. Ren, T Chou, Carbon nanotube/carbon fiber hybrid multiscale composites, J. Appl. Phys. 91 (9) (2002) 6034–6037.
[15] T. Susi, A.G. Nasibulin, H. Jiang, E.I Kauppinen, CVD synthesis of hierarchical 3D MWCNT/carbon-fiber nanostructures, J. Nanomater. 2008 (2008) 61.
[16] J. Zhao, L. Liu, Q. Guo, J. Shi, G. Zhai, J. Song, et al., Growth of carbon nanotubes on the surface of carbon fibers, Carbon N Y 2 (46) (2008) 380–383.
[17] V.G. De Resende, E.F. Antunes, A. de Oliveira Lobo, D.A.L. Oliveira, V.J. Trava-Airoldi, E.J Corat, Growth of carbon nanotube forests on carbon fibers with an amorphous silicon interface, Carbon N Y 48 (12) (2010) 3655–3658.
[18] H. Qian, A. Bismarck, E.S. Greenhalgh, G. Kalinka, M.S Shaffer, Hierarchical composites reinforced with carbon nanotube grafted fibers: the potential assessed at the single fiber level, Chem. Mater. 20 (5) (2008) 1862–1869.
[19] F. An, C. Lu, J. Guo, S. He, H. Lu, Y Yang, Preparation of vertically aligned carbon nanotube arrays grown onto carbon fiber fabric and evaluating its wettability on effect of composite, Appl. Surf. Sci. 258 (3) (2011) 1069–1076.
[20] X. Du, H.-.Y. Liu, C. Zhou, S. Moody, Y.-.W Mai, On the flame synthesis of carbon nanotubes grafted onto carbon fibers and the bonding force between them, Carbon N Y 50 (6) (2012) 2347–2350.
[21] H. Oulanti, F. Laurent, T. Le-Huu, B. Durand, J.-.B Donnet, Growth of carbon nanotubes on carbon fibers using the combustion flame oxy-acetylene method, Carbon N Y 95 (2015) 261–267.
[22] K.L. Kepple, G.P. Sanborn, P.A. Lacasse, K.M. Gruenberg, W.J Ready, Improved fracture toughness of carbon fiber composite functionalized with multi walled carbon nanotubes, Carbon N Y 46 (15) (2008) 2026–2033.
[23] Q. An, A.N. Rider, E.T Thostenson, Electrophoretic deposition of carbon nanotubes onto carbon-fiber fabric for production of carbon/epoxy composites with improved mechanical properties, Carbon N Y 50 (11) (2012) 4130–4143.
[24] Z. Zhao, K. Teng, N. Li, X. Li, Z. Xu, L. Chen, et al., Mechanical, thermal and interfacial performances of carbon fiber reinforced composites flavored by carbon nanotube in matrix/interface, Compos. Struct. 159 (2017) 761–772.
[25] H. Yao, X. Sui, Z. Zhao, Z. Xu, L. Chen, H. Deng, et al., Optimization of interfacial microstructure and mechanical properties of carbon fiber/epoxy composites via carbon nanotube sizing, Appl. Surf. Sci. 347 (2015) 583–590.
[26] Q. Li, J.S. Church, M. Naebe, B.L Fox, A systematic investigation into a novel method for preparing carbon fibre–carbon nanotube hybrid structures, Compos. Part A: Appl. Sci. Manuf. 90 (2016) 174–185.
[27] Q. Li, J.S. Church, M. Naebe, B.L Fox, Interfacial characterization and reinforcing mechanism of novel carbon nanotube–carbon fibre hybrid composites, Carbon N Y 109 (2016) 74–86.
[28] J.N. O'Shea, J.B. Taylor, J.C. Swarbrick, G. Magnano, L.C. Mayor, K Schulte, Electrospray deposition of carbon nanotubes in vacuum, Nanotechnology 18 (3) (2007) 035707.
[29] A. Jaworek, Electrospray droplet sources for thin film deposition, J. Mater. Sci. 42 (1) (2007) 266–297.
[30] M.R. Zakaria, H.M. Akil, M.H.A. Kudus, S.S.M Saleh, Enhancement of tensile and thermal properties of epoxy nanocomposites through chemical hybridization of carbon nanotubes and alumina, Compos. Part A: Appl. Sci. Manuf. 66 (2014) 109–116.

[31] K.H. Hung, W.S. Kuo, T.H. Ko, S.S. Tzeng, C.F Yan, Processing and tensile characterization of composites composed of carbon nanotube-grown carbon fibers, Compos. Part A: Appl. Sci. Manuf. 40 (8) (2009) 1299–1304.
[32] M.R. Zakaria, M.H. Abdul Kudus, H. Md Akil, M.Z.M. Thirmizir, M.F.I. Abdul Malik, M.B.H. Othman, et al., Comparative study of single-layer graphene and single-walled carbon nanotube-filled epoxy nanocomposites based on mechanical and thermal properties, Polym. Compos. 40 (S2) (2019) E1840–E18E9.
[33] K.J. Kim, J. Kim, W.-.R. Yu, J.H. Youk, J Lee, Improved tensile strength of carbon fibers undergoing catalytic growth of carbon nanotubes on their surface, Carbon N Y 54 (2013) 258–267.
[34] E. Moaseri, M. Karimi, M. Maghrebi, M Baniadam, Two-fold enhancement in tensile strength of carbon nanotube–carbon fiber hybrid epoxy composites through combination of electrophoretic deposition and alternating electric field, Int. J. Solids Struct. 51 (3–4) (2014) 774–785.
[35] H. Mei, S. Zhang, H. Chen, H. Zhou, X. Zhai, L Cheng, Interfacial modification and enhancement of toughening mechanisms in epoxy composites with CNTs grafted on carbon fibers, Compos. Sci. Technol. 134 (2016) 89–95.
[36] D.C. Davis, J.W. Wilkerson, J. Zhu, V.G Hadjiev, A strategy for improving mechanical properties of a fiber reinforced epoxy composite using functionalized carbon nanotubes, Compos. Sci. Technol. 71 (8) (2011) 1089–1097.
[37] E. Moaseri, M. Karimi, M. Maghrebi, M Baniadam, Fabrication of multi-walled carbon nanotube–carbon fiber hybrid material via electrophoretic deposition followed by pyrolysis process, Compos. Part A: Appl. Sci. Manuf. 60 (2014) 8–14.
[38] S. Rahmanian, K.S. Thean, A.R. Suraya, M.A. Shazed, M.A. Mohd Salleh, H.M Yusoff, Carbon and glass hierarchical fibers: influence of carbon nanotubes on tensile, flexural and impact properties of short fiber reinforced composites, Mater. Des. 43 (2013) 10–16.
[39] E.J. Garcia, B.L. Wardle, A. John Hart, N Yamamoto, Fabrication and multifunctional properties of a hybrid laminate with aligned carbon nanotubes grown In Situ, Compos. Sci. Technol. 68 (9) (2008) 2034–2041.
[40] M. Li, Y. Gu, Y. Liu, Y. Li, Z Zhang, Interfacial improvement of carbon fiber/epoxy composites using a simple process for depositing commercially functionalized carbon nanotubes on the fibers, Carbon N Y 52 (2013) 109–121.
[41] K. Naito, J.-.M. Yang, Y. Xu, Y Kagawa, Enhancing the thermal conductivity of polyacrylonitrile-and pitch-based carbon fibers by grafting carbon nanotubes on them, Carbon N Y 48 (6) (2010) 1849–1857.
[42] B. Wang, Q. Fu, T. Yin, H. Li, L. Qi, Y Fu, Grafting CNTs on carbon fabrics with enhanced mechanical and thermal properties for tribological applications of carbon fabrics/phenolic composites, Carbon N Y 139 (2018) 45–51.